AGU PUBLICATIONS

JGR

Journal of Geophysical Research: Oceans

RESEARCH ARTICLE

10.1002/2014JC010564

# Whales and waves: Humpback whale foraging response and the shoaling of internal waves at Stellwagen Bank

**Jesús Pineda[1], Victoria Starczak[1], José C. B. da Silva[2], Karl Helfrich[3], Michael Thompson[4], and David Wiley[4]**

[1]Biology Department, Woods Hole Oceanographic Institution, Woods Hole, Massachusetts, USA, [2]Interdisciplinary Centre of Marine and Environmental Research and Department of Geosciences, Environment and Spatial Planning, University of Porto, Porto, Portugal, [3]Department of Physical Oceanography, Woods Hole Oceanographic Institution, Woods Hole, Massachusetts, USA, [4]National Oceanic and Atmospheric Administration/Office of National Marine Sanctuaries, Stellwagen Bank National Marine Sanctuary, Scituate, Massachusetts, USA

**Key Points:**
- Internal waves regularly approach a bank, which is an ecological hotspot
- At short-time scales, there was no relationship between whales and internal waves
- Large interannual variability in humpback whale sightings was observed at an ecological hotspot

**Correspondence to:**
J. Pineda,
jpineda@whoi.edu

**Citation:**
Pineda, J., V. Starczak, J. C. B. da Silva, K. Helfrich, M. Thompson, and D. Wiley (2015), Whales and waves: Humpback whale foraging response and the shoaling of internal waves at Stellwagen Bank, *J. Geophys. Res. Oceans*, *120*, 2555–2570, doi:10.1002/2014JC010564.

Received 4 NOV 2014
Accepted 9 MAR 2015
Accepted article online 18 MAR 2015
Published online 2 APR 2015

**Abstract** We tested the hypothesis that humpback whales aggregate at the southern flank of Stellwagen Bank (SB) in response to internal waves (IWs) generated semidiurnally at Race Point (RP) channel because of the presence of their preferred prey, planktivorous fish, which in turn respond to zooplankton concentrated by the predictable IWs. Analysis of synthetic aperture radar (SAR) images indicates that RP IWs approach the southern flank of SB frequently (~62% of the images). Published reports of whale sighting data and archived SAR images point to a coarse spatial coincidence between whales and Race Point IWs at SB's southern flank. The responses of whales to IWs were evaluated via sightings and behavior of humpback whales, and IWs were observed in situ by acoustic backscatter and temperature measurements. Modeling of IWs complemented the observations, and results indicate a change of ~0.4 m/s in current velocity, and ~1.5 Pa in dynamic pressure near the bottom, which may be sufficient for bottom fish to detect the IWs. However, fish were rare in our acoustic observations, and fish response to the IWs could not be evaluated. RP IWs do not represent the leading edge of the internal tide, and they may have less mass-transport potential than typical coastal IWs. There was large interannual variability in whale sightings at SB's southern flank, with decreases in both numbers of sightings and proportion of sightings where feeding was observed from 2008 to 2013. Coincidence of whales and IWs was inconsistent, and results do not support the hypothesis.

## 1. Introduction

Humpback whales are large cosmopolitan baleen whales that undertake annual migrations between high-latitude feeding areas and low-latitude calving grounds [*Clapham and Mead*, 1999; *Dawbin*, 1966]. Our study area in the Stellwagen Bank National Marine Sanctuary (SBNMS) is a seasonal feeding area where humpbacks whales aggregate to feed primarily on sand lance *Ammodytes* spp. [*Payne et al*., 1990; *Weinrich et al*., 1992], a small fish, although other species such as herring, *Clupea harengus* [*Weinrich et al*., 1997], and euphausiids *Meganyctiphanes norvegica* [*Stevick et al*., 2008], are also consumed. Within the SBNMS, the local abundance of humpback whales fluctuates with local sand lance abundance [*Payne et al*., 1990; *Weinrich et al*., 1992] and humpback feeding behavior varies relative to sand lance behavior. For example, humpbacks feed along the bottom at night when sand lance bury in the substrate [*Friedlaender et al*., 2009; *Hazen et al*., 2009; *Ware et al*., 2014] and use bubble nets to forage in the upper portions of the water column during the day when sand lance leave the substrate to feed [*Friedlaender et al*., 2009; *Wiley et al*., 2011]. In addition, the geographic distribution of feeding humpback whales within the SBNMS varies on a temporal basis ranging from hours to months, and these feeding locations are also thought to be highly influenced by sand lance aggregations.

Sand lance *Ammodytes* spp. are preyed upon by humpback whales in Stellwagen Bank (SB) waters [*Auster et al*., 2006; *Garrison and Link*, 2000]. Two species of sand lance occur in this region, *Ammodytes americanus* and *A. dubius*. Adults burrow into sandy habitats at night and emerge during the day to form schools and feed in the water column on copepods and other zooplankton [*Robards et al*., 1999]. Sand lance abundances can be high, accounting for 50% of trawl biomass in some years [*Auster et al*., 2006]. Variability in abundance has been linked to whale distributions and movements on SB and the Gulf of Maine [*Friedlaender et al*., 2009],

**Table 1.** Types of Data and Dates of Data Collection[a]

| Year | Month | Day of Month for Ship Work | Temperature | Day of Month of Satellite Image |
|---|---|---|---|---|
| 2008 | May | 31 | | |
| 2008 | Jun | 1, 2, 3 | Mooring | 1, 4, 6, 10, 13, 17, 21, 23, 26 |
| | Jul | 30, 31 | | 4, 7, 9, 12, 15, 21, 18, 24, 26, 28, 31 |
| | Aug | 1 | | 1, 4, 6, 9, 17, 20, 22 |
| 2009 | Jun | 4, 7, 8 | Mooring | 4, 8, 11, 14, 20, 24, 27, 28 |
| | Jul | 5, 6, 7, 10 | Mooring | 6, 13, 25 |
| 2010 | Jun | 27 | Suspended | 11 |
| | Jul | 13, 23, 24, 25 | Suspended | 25, 29, 31 |
| | Aug | | | 5, 13, 14, 16, 18, 22, 29 |
| 2011 | Jun | 16, 30 | Suspended | 15, 17 |
| | Jul | 1, 16, 17 | Suspended | 12, 14, 18, 20, 29, 31 |
| 2012 | Jun | 7 | Suspended | 3, 6 |
| | Jul | 19, 20 | Suspended | 17, 20, 31 |
| | Aug | 1, 2 | Suspended | 2 |
| 2013 | Jun | 22 | Suspended | |
| | Jul | 8, 9, 21, 22 | Suspended | |

[a]CTD and acoustics data were taken on all field days, and video started on 30 July 2008.

and a switch in distribution from Stellwagen Bank (SB) to a northern locality, Jeffrey's Ledge, was related to a decrease in sand lance abundance at SB, and an increase in herring biomass at the northern locality [*Weinrich et al*., 1997].

Cetaceans and sand lance are major components of the Massachusetts Bay pelagic community. Even though the distributions of each group have changed over the decades, these organisms converge in relatively high abundance at SB's southwestern corner [Figure 58, *U.S. Department of Commerce*, 2010; *Wiley et al*., 2003]. Whale-watching boats frequent this area, and spatial density patterns of fishing trips indicate that SB southern flank is an area of high use by the commercial fishing industry to catch fish and invertebrates [Chapter 4, *U.S. Department of Commerce*, 2010]. Thus, SB's southern flank is a hotspot in the sense that population densities of key species are high [e.g., *Nelson and Boots*, 2008]. Hydrodynamic forcing, including non linear internal waves (NLIWs), may contribute to elevated biomass at SB.

NLIWs and internal tides are ubiquitous features in the world ocean, and studies have revealed that NLIWs and internal tidal bores have broad ecological consequences, including determination of zooplankton, ichthyoplankton, and fluorescence patchiness [*Haury et al*., 1983; *Kingsford and Choat*, 1986; *Lennert-Cody and Franks*, 1999], and zooplankton accumulation and transport [*Kingsford and Choat*, 1986; *Pineda*, 1999]. Studies on internal waves in Massachusetts Bay have focused on the nonlinear evolution of internal waves in relatively deep waters ($\sim>$ 70 m) that emanate from SB and propagate shoreward [*Chereskin*, 1983; *Halpern*, 1971; *Lai et al*., 2010a; *Scotti et al*., 2007] and their effects on bottom sediments [*Butman et al*., 2006], plankton distribution [*Haury et al*., 1983; *Lai et al*., 2010b], and the shoaling of the NLIWs [*Scotti and Pineda*, 2004; *Scotti et al*., 2008]. In the central Gulf of Maine, internal waves influence the ecology of suspension feeders [*Witman et al*., 1993]. For typical tidally generated NLIWs, large amplitude internal waves represent the leading edge of the nonlinear internal tide, and the pycnocline deepens or shallows for hours after the waves pass by. NLIWs and internal tides in Massachusetts Bay, like in other coastal environments [e.g., *Winant and Bratkovich*, 1981], are energetic in late spring and summer, when the water column is well stratified.

Synthetic Aperture Radar (SAR) detects changes in surface roughness produced by the NLIWs [*Alpers*, 1985; *da Silva et al*., 1998]. Using SAR, *da Silva and Helfrich* [2008] found that, in addition to the well-known waves that originate from SB, another set of internal wave packets propagate into Massachusetts Bay, emanating from Race Point Channel, and that Race Point waves are as common as Stellwagen Bank waves. The internal wave packet distribution mapped from SAR data indicates that NLIWs tend to affect the southern flank of Stellwagen Bank [*Clark et al*., 2006]. Although *Clark et al*. [2006] do not discuss wave origin, the analysis by da *Silva and Helfrich* [2008] points to Race Point.

Race Point internal waves propagate in two different directions: 250°T and 275°T (on average, *da Silva and Helfrich* [2008]), and wave packets that propagate toward 275°T may approach the southern tip of Stellwagen Bank. Generation of internal wave packets at Race Point Channel occurs every tidal cycle

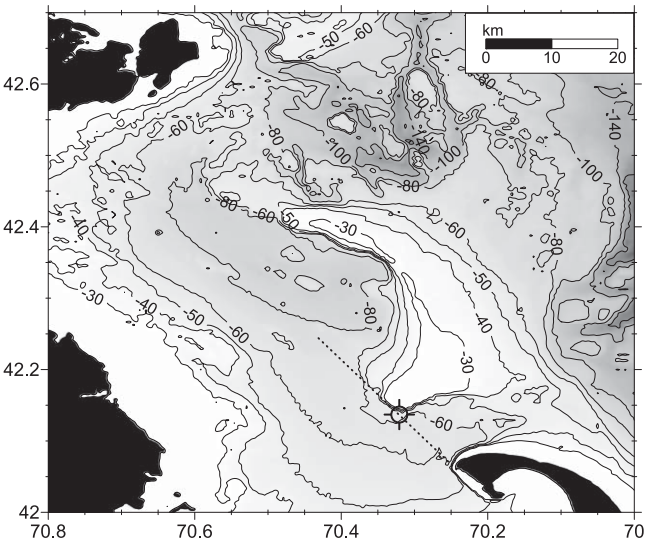


**Figure 1.** Study site. Symbol at the SB southwestern flank is the anchor station position and approximate site of 55 m temperature mooring (2008 and 2009, N 42° 08.214, W 70° 19.241). Temperature mooring was tethered off the R/V *Auk* in 2010–2013. Dashed line connects generation site at Race Point channel to field site, and line is oriented 325°T.

(every 12.4 h) during the ebb tide, before low tide at Boston and Race Point Channel. Preliminary investigation suggests that the NLIWs may be generated during the ebb phase of the tide, propagating upstream when the current speeds reach the transcritical regime (i.e., when the current speed nearly matches the phase speed of mode 1 long internal waves). These NLIWs propagate at speeds of 0.3–0.5 m/s, and would approach SB, about 10 km away from the presumed generation site, 6–9 h after low water at Boston [*da Silva and Helfrich*, 2008]. Predictability of generation and short distance between generation and shoaling sites make Stellwagen Bank southern flank a model system to investigate shoaling NLIWs and their ecological consequences. The occurrence of predictable NLIWs at SB's southern flank is suggestive, given that large predators, fish, and whales, tend to concentrate at SB [Chapter 4, *U.S. Department of Commerce*, 2010].

Internal waves [*Shanks*, 1983; *Zeldis and Jillet*, 1982] and internal bores [*Pineda*, 1999] create surface convergences that can concentrate zooplankton, and concentration in these convergences requires zooplankton to be buoyant or to swim against the currents [*DiBacco et al*., 2011; *Franks*, 1992; *Le Fèvre*, 1986]. Internal tidal bores can also transport zooplankton and larvae [*Leichter et al*., 1998; *Pineda*, 1994; *Vargas et al*., 2004], and modeling and experimental studies have addressed particle transport when the internal tidal bores can be viewed as buoyant gravity currents [*Helfrich and Pineda*, 2003; *Scotti and Pineda*, 2007]. Internal solitary waves (ISW) can transport surface plankton in deep water when transport is "aided" by wind drift or by zooplankton horizontal swimming in the direction of wave propagation [*Lamb*, 1997]. Long-distance mass transport by ISW is only possible when stratification increases toward the surface [*Lamb*, 2002].

Zooplanktivorous predators forage where plankton accumulate, including fronts [*Hamner*, 1988; *Le Fèvre*, 1986], surface slicks [*Watkins and Schevill*, 1979], and internal wave convergences (D. Wiley and J. Pineda, personal observation, 2008). Whales may prey on euphausiids concentrated by internal waves at Platts Bank in the central Gulf of Maine [*Stevick et al*., 2008], and pilot whales following an internal solitary wave in the South China Sea may have been foraging [*Moore and Lien*, 2007]. In Massachusetts Bay, during early summer, sand lance, and humpback abundance was correlated with tidal height, a proxy for various tidal processes, including tidally generated internal waves [*Hazen et al*., 2009]. However, a mechanistic linkage between internal waves and whale feeding is still missing. *Embling et al*. [2013] found that the distribution of pelagic fish was influenced by a small bank in the Celtic Sea, and suggested that internal waves generated at the small bank would influence fish abundance, although the mechanisms where nascent internal waves would influence fish abundance are unclear. Sites where convergences occur predictably because of physiographic configuration and bathymetry may be sites of intense trophic activity [*Le Fèvre*, 1986]. Stellwagen Bank is a well-known source of internal waves [*Haury et al*., 1979; *Scotti et al*., 2007], but the bank was not known as an area where NLIWs shoal frequently. Our recent SAR observations of Race Point internal waves offer a fresh picture: internal waves emanating from the tip of Cape Cod repeatedly approach the southwestern flank of Stellwagen Bank.

We tested the hypothesis that humpback whale distribution is partially determined by NLIWs, by (1) developing a better understanding of the NLIWs in the region through analyses of SAR images, field observations of the internal waves, and modeling, and (2) by testing the hypothesis through in situ

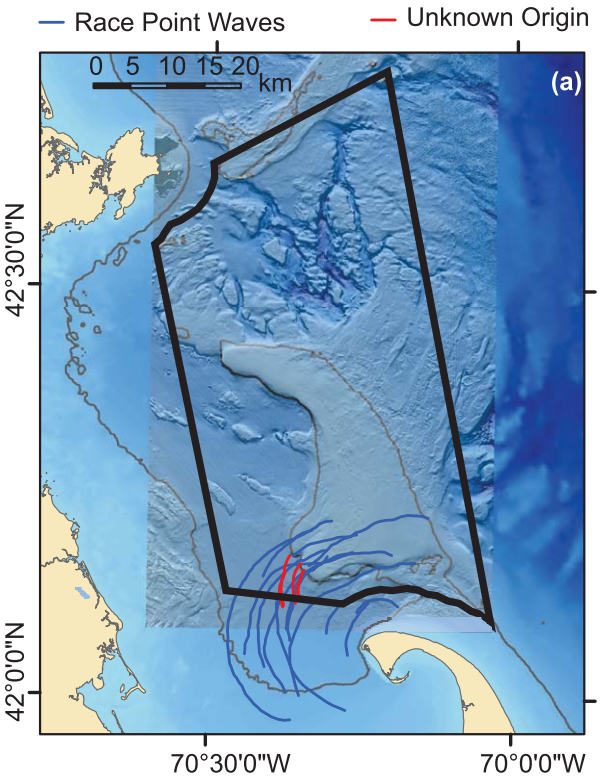


**Figure 2.** NLIWs crests from 2008 SAR images. Composite map showing positions of wave fronts observed in the 2008 TerraSAR-X satellite images. Blue shows the wave fronts identified to propagate toward 325°T, which were in collision course with the southern steep slopes of Stellwagen Bank. Red wave fronts represent waves generated at unknown locations. Heavy black line enclosing SB delineates the Stellwagen Bank National Marine Sanctuary.

observations of whale sightings and NLIWs. The two-link trophic response hypothesis postulates that schools of sand lance respond to patches of zooplankton created by predictable Race Point internal waves, and that humpback whales can take advantage of these sand lance schools. Some assumptions in this hypothesis have been supported, namely that zooplankton accumulate in NLIWs [*Zeldis and Jillet*, 1982], that sand lance feed on zooplankton [*Robards et al.*, 1999], and that whales feed on sand lance [*Hain et al.*, 1982]. On the other hand, assumptions that have not been tested include that sand lance can respond to patches of zooplankton created by NLIWs, and that humpback whales take advantage of schools of fish in IW events at Stellwagen Bank. Do Race Point IWs approach regularly Stellwagen Bank southern flank? Is there a temporal correlation between the abundance of humpback whales and the arrival of Race Point IWs at SB southern flank? Are whales more likely to feed on SB southern flank on days with NLIWs?

In section 2, we present the observational program to develop a better understanding of the NLIWs, the approach to model them, and finish with the observations and experimental design to test the hypothesis. In section 3, we describe the IWs observed with SAR and in situ, we provide a description of NLIWs from coincident SAR, acoustic, and temperature data, and then we present the modeling results. We then report on the relationship between the in situ observations of IWs and our whale sightings, and on the interannual variability of whale sightings. We finish with a discussion on acoustic observations of fish.

Section 4 discusses properties of Race Point NLIWs, differences with NLIWs observed in other coastal regions, and some ecological consequences of these differences. We then evaluate the study's hypothesis in view of our observations, discuss interannual variability in whale sightings, and consider the effects of NLIWs on fish. In section 5, we summarize our findings.

## 2. Methods

NLIWs were observed from 2008 to 2013 using SAR, temperature and acoustics (Table 1), and they were modeled using observed density profiles. The experimental design to test the hypothesis incorporated the spatial and temporal predictability of Race Point semidiurnal internal waves approaching Stellwagen Bank's southwestern flank.

In situ observations in the late springs and summers of 2008–2013 to address the hypotheses on the response of humpback whales to NLIWs included shipboard and moored measurements. Shipboard data were obtained from National Oceanic and Atmospheric Administration (NOAA) R/V *Auk* anchored south of the bank, at ~55 m water depth (Figure 1). Position changed when the R/V *Auk* pivoted around the anchor with the tidal currents. Position differences from the beginning to the end of the daily observations were up to 180 m. Tidal range in the study area is relatively large, with an average lunar-day maximum tidal range

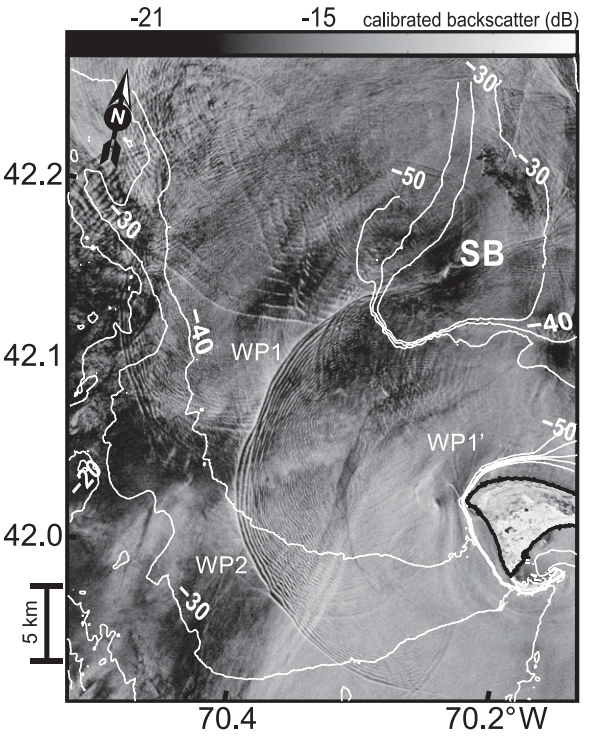


**Figure 3.** TerraSAR-X image acquired on 23 June 2008 at 22:25 h UTC over Cape Cod Bay, showing two large ISW trains emanating from Race Point Channel with bathymetry overlaid on the SAR image. A third and small "nascent" wave packet (WP1') at the expected time of generation is visible in Race Point channel.

of 3.12 m. (2008–2010 data for Boston tidal station NOAA 8443970, 60 km from our field site.) In each year from 2008 to 2013, 5–7 days of shipboard measurements were interspersed between early June and early August. Whenever possible, SAR satellite images were requested for ship days (Table 1). To minimize potential bias from whales' diurnal patterns in feeding activity, fieldwork dates were chosen to include days when IWs were expected to approach SB in the morning, noon, and midafternoon.

### 2.1. Synthetic Aperture Radar (SAR) Observations

We addressed whether NLIWs approach SB southern flank from 2008 SAR satellite data. We scheduled and analyzed 25 TerraSAR-X satellite overpasses of the study area during the period from 1 June 2008 to 22 September 2008. Of these, 4 out of 25 images were not appropriate for addressing the research objectives because sea surface wind speed was too strong or too weak, impeding detection of the surface signature of the internal waves by SAR. TerraSAR-X has a dawn-dusk orbit and thus overpasses the study region at 10:00 h or 22:00 h Coordinated Universal Time (UTC). Because our vessel measurements were conducted during the day (between 12:30 h and 22:00 h UTC), we could not obtain coincident vessel and TerraSAR-X overpass measurements. However, the ENVISAT satellite, which is capable of detecting NLIWs with the SAR and has an orbit close to noon midnight, was used to obtain an image on 31 July 2008 (at 14:40 h UTC), approximately 30 min after the first internal wave was recorded in the field (see below). The TerraSAR-X and the ENVISAT SAR images from 31 July 2008 and 3 days with field observations were used to compute a travel-time plot. Satellite data were also collected for the 2009–2012 period from June to August, inclusive, coincident with the 2009–2012 field seasons (Table 1). However, these data were not used in this contribution, and they do not change the general conclusions obtained from analysis of the 2008 data set.

### 2.2. Moored and Suspended Temperature

In late May 2008, temperature moorings were deployed at locations with water depths of 55 and 23 m at the southwestern flank of Stellwagen Bank to characterize the NLIWs. Another mooring was deployed at the Stellwagen Bank northern flank in 39 m of water. The 55 and 39 m moorings were lost after a few days of deployment, likely to trawl fishing. Subsequent mooring deployments in late July 2008 and June 2009 at the southwestern flank of Stellwagen Bank were 5–18 days, and no mooring was redeployed at the north flank. Seabird SBE39 temperature loggers were generally spaced every 4.5 m along the mooring line over the entire water column, and recorded at 20 or 40 s intervals, with buoyancy provided by rigid subsurface buoys. SBE39 and RBR 2050 temperature and pressure sensors at the submerged buoys were used to estimate mooring bending by currents. On some deployments, an Onset Computer Corporation HOBO TempPro temperature logger attached to a surface float was tethered to the top of the mooring. These surface loggers recorded temperature every 140 s, although the response time of the HOBO TempPro is slower than 140 s.

Beginning in 2010, temperature was recorded using 26 RBR 1060 temperature loggers attached to a ~53 m long line suspended from a large float, recording at 10 s intervals. Most temperature loggers were spaced 2.25 m apart, but the two top subsurface loggers had shorter separations, from 0.5 to 2 m, depending on the

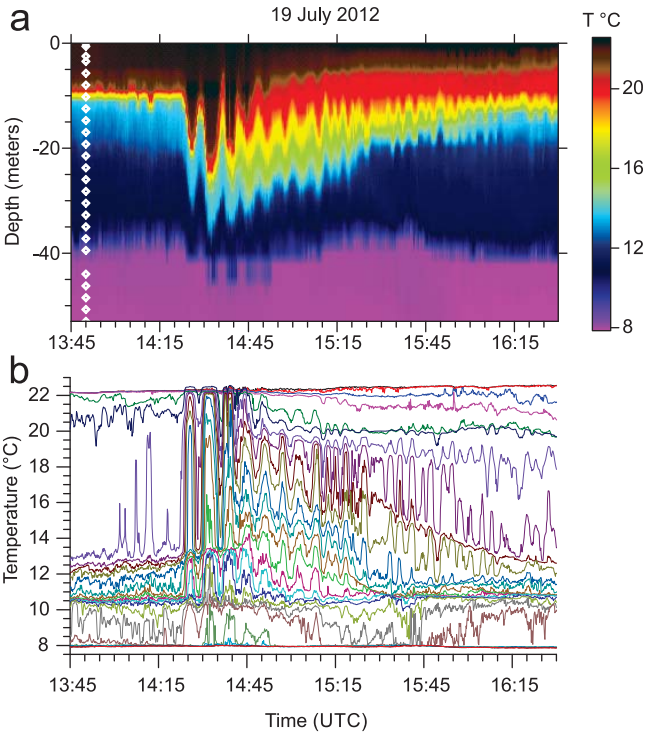


**Figure 4.** NLIWs recorded on 19 July 2012 using temperature data. The temperature loggers were fixed to a line suspended from a large float. (a) Interpolated temperature; white symbols depict temperature logger positions. (b) Raw temperature measured at 10 s intervals from individual loggers. Bottom logger is < 3 m above bottom. Predicted low tide time at Boston light station is 10:05 h UTC.

configuration of the top of the mooring. The float was tethered to the boat, and the temperature string was held taunt by suspended weights at the bottom of the line.

### 2.3. Hydrographic, Acoustics and Video Shipboard Observations

Shipboard measurements included Conductivity, Temperature, and Depth profiler (CTD) casts, single-beam or dual-beam 200 and 120 kHz acoustic backscatter (Biosonics DTX), and live underwater video (Splash-Cam Deep Blue) with underwater flashlights fitted with light diffusers. Acoustic and video data acquisition started in July 2008, when a single 200 kHz frequency unit was available, with use of dual frequencies 120 and 200 kHz starting in 2010. One or two acoustic transducer heads were deployed from the stern at about 1 m depth. Data were fed to a PC, and acoustic scatter dynamics were observed in real time. Acoustic backscatter data were used to detect fish and NLIWs, and the identity of acoustic backscatter "patches" and "traces" was assessed with the underwater live camera by positioning the camera at the depth of observed acoustic patches. The video camera was attached to a caged Seabird SBE19 CTD or to other weighty objects, and depth of the video camera was estimated from line out (line marked every 10 meters), and occasionally from the camera's acoustic return in the echograms. Acoustic patches and traces were assigned to a fish species when video images were positively identified. Video was saved in compressed format. Quantification of sand lance was not attempted in this study because identification of all acoustic patches was not possible. Moreover, the number of sand lance schools positively identified with the live video camera at the time of NLIW occurrence was very small, and this low number precluded evaluating rigorously the response of fish to the NLIWs.

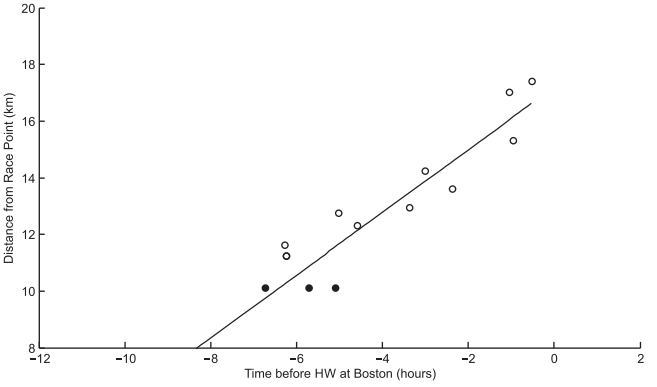


**Figure 5.** Travel-time graph based on 2008 SAR images and field observations. The vertical axis represents the distance of leading internal solitary waves in each packet measured from Race Point (42.06° N, 70.25° W) along a propagation axis with direction 325°T. Open symbols represent points where the wave fronts in the SAR intersect the propagation axis, whereas closed symbols are arrival time of the NLIWs to mooring location (on June 2008 data). Times are relative to high tide (HW) at Boston Harbor. (Negative times represent time before high tide.) The slope of the linear fit provides an average of propagation speeds in direction 325°T ($c = 0.31$ m/s).

### 2.4. Modeling

Observations were complemented with a mathematical model of large-amplitude internal solitary waves to investigate potential changes in circulation and pressure through the water column induced by the waves. Measured ambient density structure (i.e., stratification) was used to compute

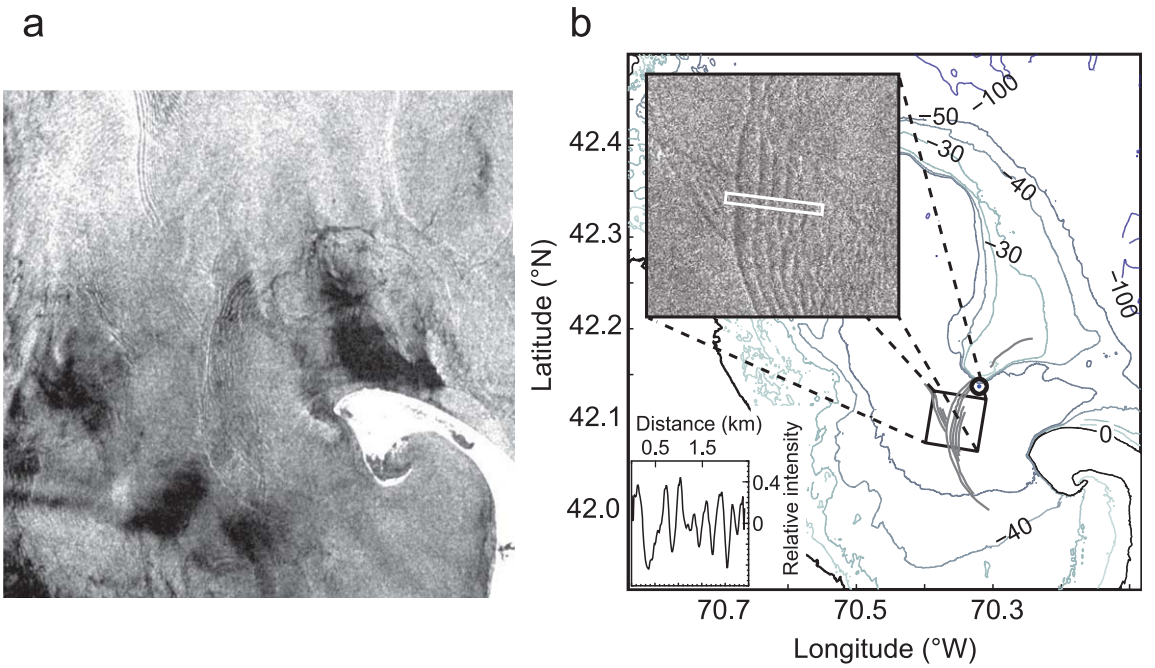


**Figure 6.** (a) ENVISAT SAR image 31 July 2008 acquired at 2:29 h UTC. (b) Schematic representation of internal wave fronts in Massachusetts Bay shown with wave length calculated from the image. The dark circle at the southwestern flank of SB is location of RV *Auk* when the image was acquired. Axes in inset are distance (x, in km), and relative intensity (y).

internal solitary waves using the fully nonlinear, Dubreil-Jacotin-Long (DJL) equation [see *Helfrich and White*, 2010; *Stastna and Lamb*, 2002]:

$$\frac{\partial^2\eta}{\partial x^2}+\frac{\partial^2\eta}{\partial z^2}+\frac{N^2(z-\eta)\eta}{c^2}=0 \tag{1}$$

Here $\eta(x,z)$ is the displacement of a streamline (i.e., isopycnal) from its resting position (i.e., its position far ahead and behind the wave) where $\eta = 0$, $N^2(z) = -(g/\rho_{00})d\rho_0(z)/dz$ is the Brunt-Väisälä frequency based on the background density profile $\rho_0(z)$, $\rho_{00}$ is a reference density, $g$ is the gravitational acceleration, and $c$ is the phase speed of the wave. For a given observed background density field, we computed "families" of wave solutions using the Newton-Raphson method. These families are described by continuous curves that relate wave speed $c$ to the wave amplitude $\eta_0$, = max[$\eta(0,z)$] (or min depending on sign of $\eta$). Solutions of this equation were used to compute the wave-induced horizontal, $u=c\eta_z$, and vertical, $w=-c\eta_x$, velocity fields and the dynamic pressure (found after removing the hydrostatic pressure due to the background density field):

$$p_{\mathrm{dyn}}(x,z)=\frac{c^2}{2}\left[1-\left(\eta_x^2+\eta_z^2\right)\right]-\rho_0(z-\eta)g\eta \tag{2}$$

Wave-induced velocities and dynamic pressures were calculated at maximum depths where fish that may respond to surface intensified internal waves can be found (near the bottom).

### 2.5. Whale Sightings and Behavior

Whale sightings and whale behavior were recorded by two trained biologists on opposite sides of the R/V *Auk*'s raised observing platform. Each observer scanned 180° of the horizon for 5 min every 15 min for 5.5–10 h while the vessel was anchored on station. Whales were located (distance, bearing) with Leica Vector Viper II binoculars, which feature a digital compass and a laser rangefinder for measuring distance up to 4000 m. Number, behavior, and location of whales were told to a third person who immediately recorded the data on an electronic tablet. Behaviors were categorized as feeding, logging, swimming, diving, fluking, breaching, aerobatics, motionless, other, and unknown [*Weinrich and Kuhlberg*, 1991; *Weinrich et al*., 1992]. Feeding included lobtailing, a feeding mode where humpback whales use their tail flukes to hit surface waters [*Weinrich et al*., 1992]. When several whales were observed together and at least one whale was feeding, the behavior for that sighting was recorded as feeding.

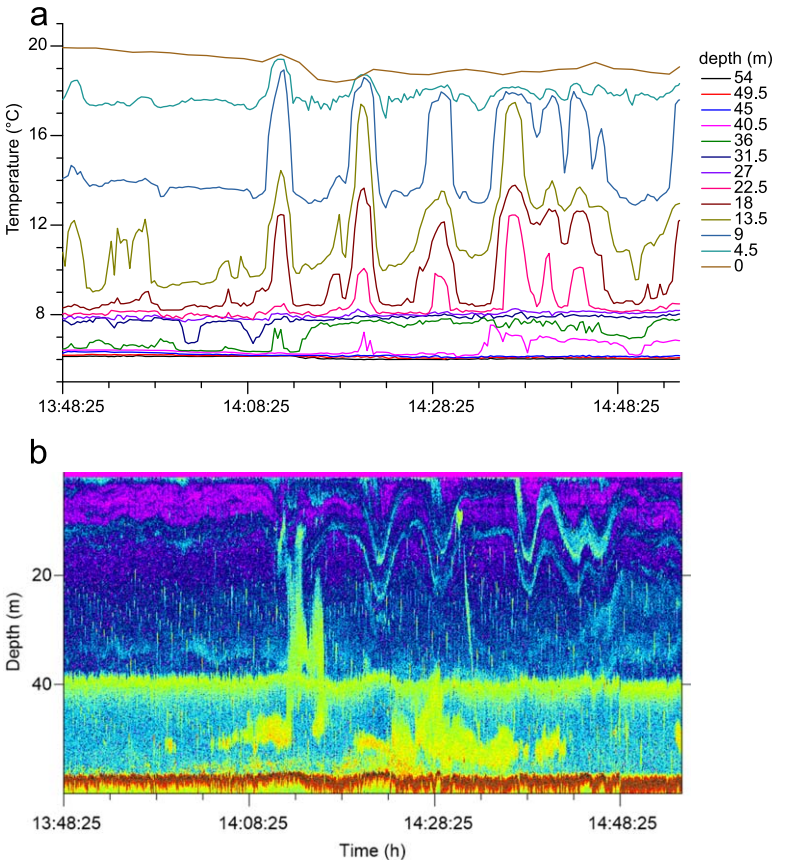


**Figure 7.** Internal waves from raw temperature and acoustic backscatter on 31 July 2008. (a) Coincident temperature variability reveal the NLIWs; depth is in meters, time is UTC, and measurement interval is 20 s. (b) Internal wave train from acoustic backscatter. Separation between ship anchored position and mooring in Figure 7(top) is ∼240 m. Station position for Figure 7 (bottom) is depicted in Figure 1. Backscatter arising with the internal wave (ca. 14:10 h) was sand lance which were identified with an underwater camera. The sharp acoustic band at ∼ 40 m is a measurement artifact.

## 3. Results

### 3.1. Internal Waves at the Southwestern Flank of Stellwagen Bank: SAR Observations

The origin and frequency of internal waves approaching SB's southwestern flank were investigated with SAR images. Observations from 2008 indicate that the majority of internal waves approaching SB's southwestern flank originate at Race Point (Figure 2). Figure 3 shows a TerraSAR-X image of Cape Cod Bay on 23 June 2008 with a nominal spatial resolution of 3 m. It reveals spatial detail of trains of NLIWs. Two semicircular wave trains of considerable lateral extension (WP1 and WP2 in the figure, coherent crest lengths of about 15 km each) can be identified. These waves were generated at Race Point channel during the ebb phase of the tide, where a nascent wave train is present (WP1'). At SB's southwestern flank, Race Point internal waves had long crests, with an observed coherent crest length of 19 km, and up to 28 km in a location 1.2 km distant from our field site (31 July 2008 SAR image, see below). Analysis of the full horizontal structure of the Race Point Channel internal wave trains in 2008 using 21 SAR images revealed that NLIW packets approached the south flank of Stellwagen Bank in 13 out of 21 images (61.9%). In 4 out 21 cases (19.1%), NLIWs did not approach SB, and in 4 other cases, NLIWs were not generated.

Moored and shipboard measurements at SB's southwestern flank detected internal wave packets. Out of 32 field days of shipboard measurements, we detected NLIWs consistent with Race Point origin in 22 cases (68.8%), no NLIWs on 4 occasions (12.5%), and NLIWs from ambiguous or non-RP origin in 6 cases (18.8%). In 2008 and 2009, NLIWs were identified at the 55 m mooring, and sometimes at the 23 m mooring. However, for various events, the data from the 23 m mooring did not reveal the internal waves observed at the 55 m mooting (results not shown). The Race Point origin of NLIWs at SB from in situ measurements was determined from the timing of the internal wave train. This considered the expected time of generation of internal waves at Race Point (low tide), and assumed for packets propagating 275°T (WP1 Figure 3), a propagation speed of 35 cm/s and 8 h later arrival to our anchor and mooring stations about 10 km away from the generation site. For packets propagating 250°T, a propagation speed of 39 cm/s and 7:10 h later arrival to our anchor station was assumed [*da Silva and Helfrich*, 2008].

The waves propagating 250°T are less likely to affect Stellwagen Bank. Estimates of arrival time can vary ± 2 h for the two wave trains because of, for example, stratification and tidal current variability. On 19 July 2012, temperature sensors fixed to the line attached to the surface float recorded NLIWs with up to ∼14 m

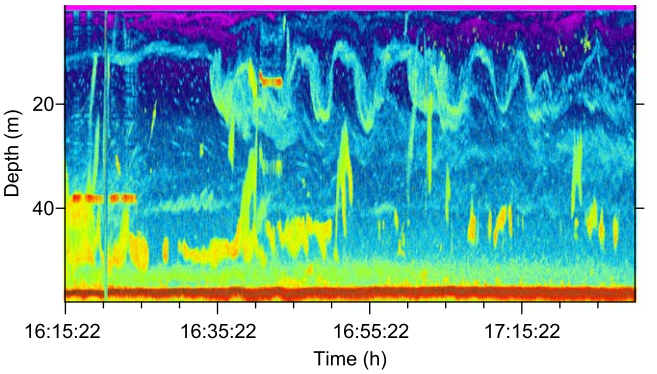


**Figure 8.** Internal wave train from acoustic backscatter on 1 August 2008. Backscatter arising with the internal wave (~16:37 h) was identified with an underwater camera as sand lance. The strong acoustic returns at 38 m at ~ 16:17 h and at 15 m at ~ 16:40 h are the video camera.

amplitude (Figure 4). As in other typical Race Point wave events, average thermocline depth changed little after the event, and thermocline depth returned to the unperturbed level.

To further assess the propagation speed of NLIWs along a line between Race Point and our field site at SB's southwestern flank (Figure 1, line heading 325°T off Race Point), we calculated propagation speed by plotting distance from Race Point as a function of time before high tide in Boston Harbor. Figure 5 presents a travel-time graph relating position and time of each wave train in 2008. The slope of the linear fit to the data gives the average propagation speed of the NLIWs, which for 325°T heading is 0.31 cm/s, in agreement with *da Silva and Helfrich* [2008]. On occasion in situ and SAR observations registered two consecutive internal wave trains; these characteristic events will be described in another paper. Last, our in situ and satellite observations also detected internal waves that generated at unknown locations (wave fronts in red color, Figure 2).

### 3.2. Coincident Satellite, Temperature, and Acoustic Backscatter Observations

A train of Race Point NLIWs identified with ENVISAT SAR on 31 July 2008 was at least 19 km in coherent crest length (Figure 6). The timing of the NLIWs suggests that they emanated from Race Point, and this was supported by the coincident SAR remote observations. In this event, the propagation speed of the NLIWs along their main axis of propagation (275°T) [*da Silva and Helfrich*, 2008], was 0.68 m/s.

Temperature data from the 55 m mooring revealed the set of internal waves (Figure 7a). From the surface to about 40 m down, the temperature varied in response to the waves. Acoustic backscatter, measured from the anchored boat 240 m distant from the temperature mooring, also revealed the event, recording internal waves by the distortion of horizontal layers of sound-scattering particles (Figure 7b). Acoustic backscatter patterns suggest vertical displacements of sound-scattering particles associated with the internal waves up to 20 m (~14:23 h, Figure 7b). A large acoustic patch in the echogram at 50 m and about 14:08 h (Figure 7b) appears to move up coincident with the arrival of the first internal wave depression. Acoustic patches return to near the bottom after the initial internal wave depressions.

On 1 August 2008, NLIWs were identified using the temperature mooring data; the wave train influenced temperature from 27 to 4.5 m water depth (results not shown). The echogram shows a set of up to seven large wave depressions (Figure 8). Acoustic patches were detected near the bottom prior to arrival of the internal waves (40–50 m, 16:15 h). Some patches appear to move to the upper water column coincident with the first and second wave depressions, and then appear to return to near the bottom, with fewer excursions to the upper water column after the first and second depressions. At ~16:51 h, an acoustic patch follows a vertical pattern that suggests fish swimming up to just above the middle of the water column under a wave crest, and then swimming down.

### 3.3. Modeling

Density profiles observed on 31 July 2008 (Cast 1) and 01 August 2008 (Cast 5) (Figure 9) were used to compute internal solitary wave solutions using the DJL equation (1). The profiles were first fit to smooth functions (dashed lines) to facilitate the calculation since both profiles exhibited density overturn representative of transient disturbances. Figure 10 shows the families of waves for Cast 1 (solid) and Cast 5 (dashed). Figure 10a shows the wave phase speed as a function of the wave amplitude $\eta_0$. Note that for both cases the waves are waves of depression, $\eta_0 < 0$, since the displacement fields $\eta(x,z)$ are similarly negative. Also shown are the peak wave-induced horizontal velocity (Figure 10b) and dynamic pressure (Figure 10c) from the DJL solutions evaluated at 1 m above the bottom. These extremes occur at the wave crest (or trough for these waves of

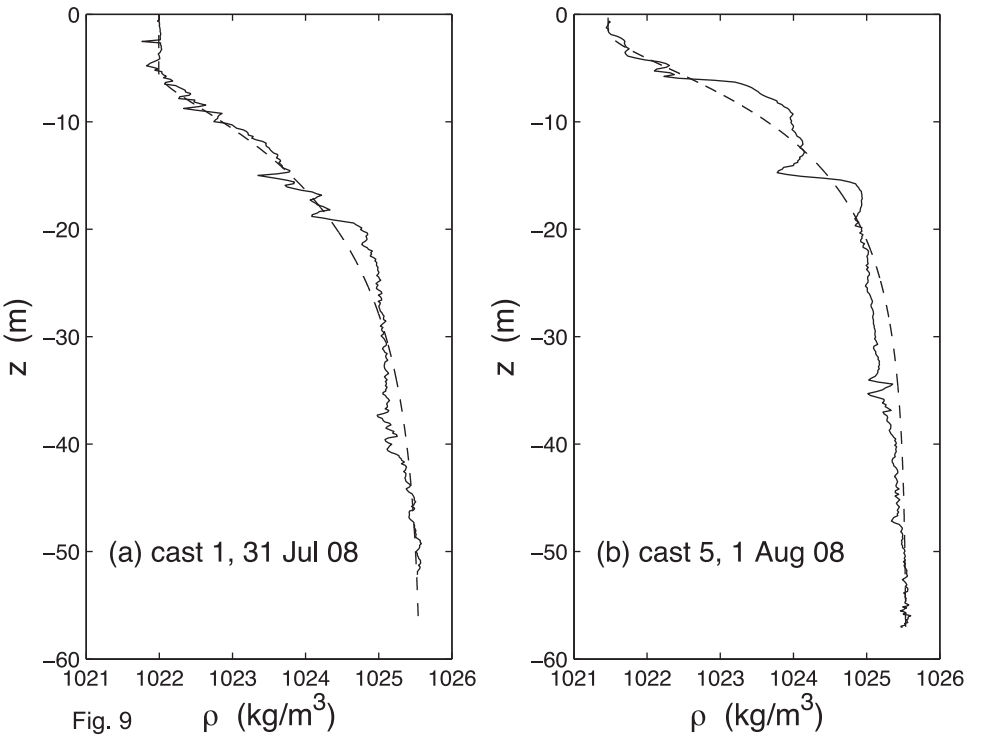


**Figure 9.** Density profiles for (a) cast 1, 31 July 2008 and (b) cast 5, 1 August 2008. The solid lines show the observed profiles with evidence of overturns. The dashed lines give the smooth fits used to compute the waves with the DJL equation.

depression). An example of a wave solution from Cast 1 with amplitude $\eta_0 = -14.1$ m is shown in Figure 11. The figure shows the density field and the horizontal velocity and dynamic pressure at 1 m above the bottom in a reference frame moving with the wave phase speed $c = 0.595$ m/s. This wave is representative of the large waves in the Race Point area, which induce peak bottom velocities of about 0.3–0.5 m/s and pressure fluctuations of about 1–2 Pa.

### 3.4. Relationship of Waves and Humpback Whale Feeding From In Situ Observations

On 2 June 2008, the predicted arrival time of Race Point waves was 15:10 h UTC. In situ whale sightings indicate that whale abundance peaked at that time (Figure 12). As there were no coincident temperature data (the temperature mooring was lost), internal waves were identified by their surface manifestation, propagating surface slicks. Humpback whales were observed swimming along internal wave slicks. Sand lances were observed swarming near the surface, and a large proportion of observed whales displayed feeding behaviors. Although this event is suggestive of an association between feeding humpback whales and internal waves, other data indicate that there is no association between whales and NLIWs. The proportion of days with detected internal waves and at least one sighting of whale feeding (15 out of 28 days from 2008 to 2013) did not differ from the proportion of days with internal waves and no whale feeding sightings (13 out of 28 days) (chi-squared = 0.143, p = 0.705, df = 1). However, whales were rare in some years (see below).

### 3.5. Interannual Variability in Whale Sightings and Behavior

In situ whale sighting observations at Stellwagen Bank's southern flank showed large interannual variability in sighting number, with abundant sightings in 2008, 2009, and 2012 but many fewer in 2010, 2011, and 2013 (Figure 13a). Total number of whale sightings on each day was weighted by the number of hours that observations were made on each day to form a simple measure of sightings per unit effort (sightings per hour per day). Mean sighting rates varied significantly between years (one-way ANOVA; square root transformed data, $F_{5,27} = 16.07$, $p < 0.001$). Mean sighting rates in years 2008, 2009, and 2012 did not differ from each other, but each of these years was significantly higher than the means in 2010, 2011, and 2013. Mean sighting rates in 2010, 2011, and 2013 were not significantly different from one another (Turkey's honestly significant difference (HSD) test, alpha = 0.05).

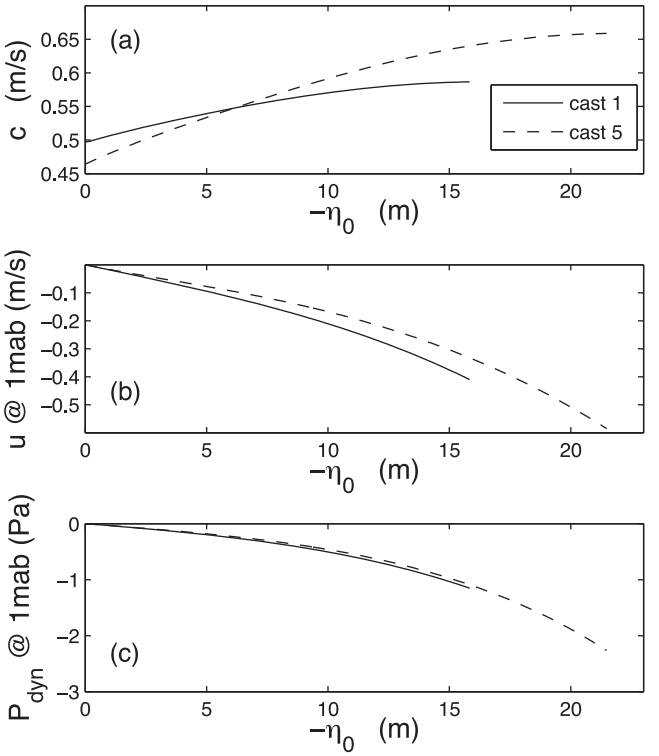


**Figure 10.** DJL model solutions for (a) wave phase speed $c$, (b) wave induced horizontal velocity $u$ at 1 m above the bottom, and (c) dynamic pressure $p_{dyn}$ at 1 m above the bottom as functions of wave amplitude $\eta_0$. Cast 1 (solid) and cast 5 (dashed).

The number of feeding observations relative to the total number of sightings on each day (termed feeding ratio) was computed to estimate the proportional number of whales that were feeding. The feeding ratio decreased from 2008 to 2010, increasing again in 2011, 2012, and 2013 (Figure 13b). Mean feeding ratio was significantly different between years (one-way ANOVA on square root transformed data, $F_{5,27} = 2.72$, $p = 0.041$). Feeding ratio was significantly higher in 2008 than in 2010 (Turkey's HSD test). No other paired comparisons between years showed significant differences. Higher feeding ratios corresponded to higher sighting rates in 2008, indicating that in 2008 when humpback whales were abundant (9.4–20.3 sightings per hour per day, average 13.7), a large proportion of these whales were feeding (4%–38%, average 24%; Figure 14). In 2010, few whales were sighted (0–1.71 sightings per hour per day, average = 0.82), and a lower number of these were feeding (0–8%, average 2%). There is very large variability in these data, however, particularly for 2009, 2012, and 2013.

### 3.6. Fish Observations

Echosounder observations were not designed to assess the abundance of sand lance and other fish. Nonetheless, our observations suggest large acoustic patches consistent with sand lance were common in 2008 and present in 2012, but rare or absent in 2010, 2011, and 2013. Sand lance in 2008 and 2012 were seen with the camera near the bottom, and our data indicates that they can swim to near the surface in the presence and in the absence of NLIWs. In 2013, we observed large schools of herring and small mackerel, identified with the camera. In 2009 and 2010, spiny dogfish (small sharks) were abundant, and these observations will be described in another paper.

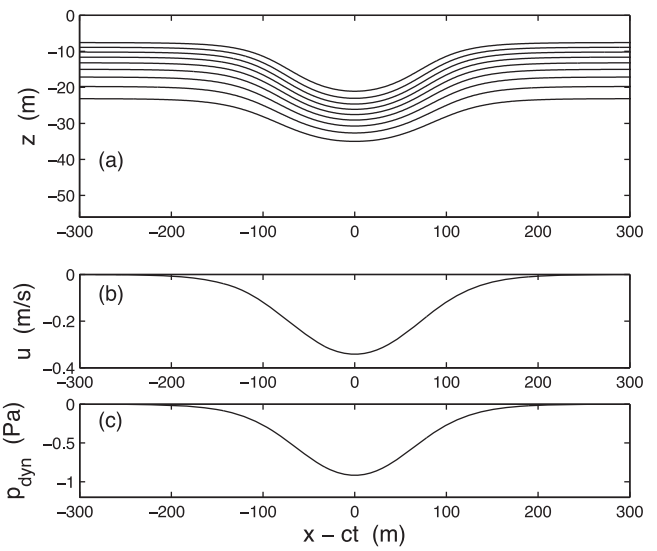


**Figure 11.** Full wave solution for Cast 1 (July 31), for a wave with phase speed $c = 0.585$ m/s and amplitude $\eta_0 = -14.1$ m. (top) Isopycnal field (contours from 1022.3 to 1024.7 kg/m$^3$ in intervals of 0.3) in a frame moving with the wave, $x - ct$. The bottom two plots show the associated wave-induced horizontal velocity and dynamic pressure at 1 m above the bottom.

## 4. Discussion

Observations of coastal NLIWs generated at Stellwagen Bank and observed in other coastal regions indicate that these waves represent the leading edge of the internal tide: thermocline depth increases or decreases after the passage

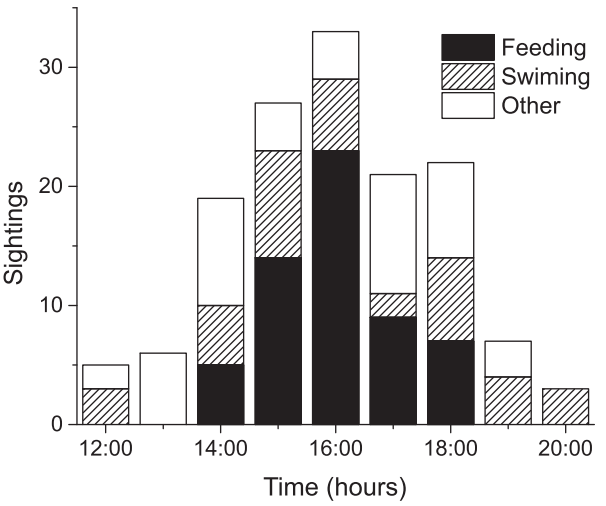


**Figure 12.** Humpback whale sightings and behavior by time of day, 2 June 2008, UTC (16:00 UTC = 12:00 local). Whale counts and behavior observed from the R/V *Auk*.

of the internal wave train, and these thermocline depth changes persist for several hours. Some features evolve as internal tidal bore warm fronts, which are capable of concentrating zooplankton, and therefore of potentially eliciting a predator foraging response. In these events, the generation of the NLIWs is in phase with the generation of the nonlinear internal tide. In most Race Point internal wave events, however, we did not observe a change in mean thermocline depth lasting a few hours associated with the waves (e.g., Figure 4). This may be due to the generation mechanism of Race Point waves. Generation is predicted to be out of phase with the internal tide [*da Silva and Helfrich*, 2008]. NLIWs that lead the internal tide sometimes evolve into internal bore warm fronts, with some characteristic features of gravity currents, including a head where current speed $u$ can be larger than propagation speed $c$, and with capability for accumulation and transport of zooplankton [*Helfrich and Pineda*, 2003; *Pineda*, 1999; *Scotti and Pineda*, 2007]. However, no circulation or zooplankton data are available for 2008, and it is not clear whether $u > c$ in typical Race Point shoaling NLIWs, or whether zooplankton are accumulated in these NLIWs. At SB's southwestern flank, typical Race Point disturbances are localized NLIWs, not gravity currents, and therefore these Race Point NLIWs have limited mass transport potential. Furthermore, the model calculations of NLIWs show that no trapped cores, where $u > c$, can occur for the stratification conditions in Figure 9 [*Helfrich and White*, 2010]. We speculate that NLIWs generated at Race Point channel are not associated with gravity currents, and have less potential for accumulation and transport than internal tidal bore warm fronts. Race Point NLIWs, however, may influence the benthic environment by producing changes in near bottom currents and dynamic pressure (Figure (10 and 11)).

Our results do not support the hypotheses that humpback whale distribution is partially determined by NLIWs, and that whales take advantage of sand lance schools that respond to predictable accumulation of zooplankton by the NLIWs. The association between whales and NLIWs is, at best, inconsistent. Although Race Point NLIWs affect an area where humpback and other baleen whales aggregate [Figure 2, and *Wiley et al*., 2003], and humpback whales were observed feeding on zooplanktivorous fish near NLIWs (Figure 12), for the large majority of observed NLIW events we found no evidence of humpback whale aggregation in response to the NLIWs. Moreover, on days with NLIWs, there were no difference between the proportion of days with no sightings of feeding humpback whales, and the proportion of days with at least one sighting of feeding humpback whales. Several processes may account for the disconnection between feeding whales and NLIWS, including no zooplankton accumulation in the NLIWs, no fish response to the NLIWs, humpback whale inability to predict the NLIWs, and little benefit for whales to forage in NLIWs because, for example, there are few prey for the whales. Whale and prey spatial and temporal variability is another obvious candidate for explaining the disconnection. Humpback whale spatial and temporal distribution at Stellwagen Bank is strongly dependent on sand lance variability [*Friedlaender et al*., 2009; *Hazen et al*., 2009]. Whereas NLIWs approaching SB are predictable in spring and summer, prey abundance varies. With no prey to attract humpback whales to a given area, a direct relationship between physical forcing by NLIWs and whale response should not be expected.

There was ample interannual variability in the number of humpback whale sightings at the field site (Figure 13). Whereas our measurements were limited in time and space, informal communications with whale-watching fleet naturalists and blogs concurrent with our field observations suggest that when humpback whales were rare at our field site at the southwestern flank of SB, groups of whales were seen feeding in other areas of Massachusetts Bay and outer Cape Cod. Humpback whale interannual sighting variability from 2008 to 2013 at our field site may be related to prey variability, and these results are consistent with

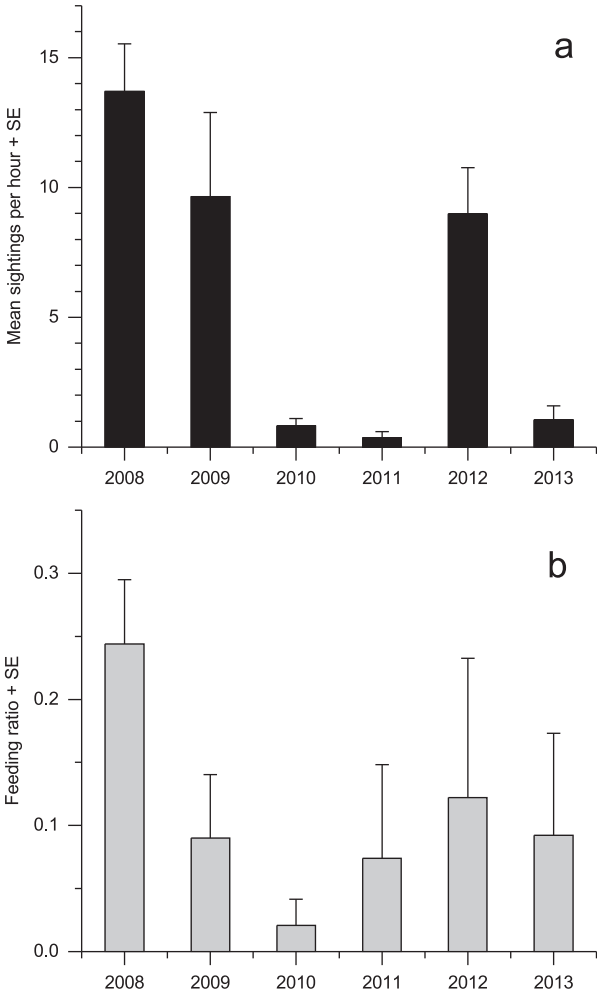


**Figure 13.** (a) Humpback whale sighting rates (whales sighted per hour) at SB's southern flank. Data are 7–9 h of daylight observations per day, average of 5–7 days in June–August of 2008–2013. Error bars are standard error. (b) Feeding ratio (number of feeding observations relative to the total number of sightings) at SB's southern flank. Data as in (a) above. Error bars are standard error.

previous studies indicating that humpback whale abundance fluctuates with local sand lance abundance [*Payne et al*., 1990; *Weinrich et al*., 1992]. When whales were very rare in 2010, there were few sightings of feeding, but in 2008 when whale sighting numbers were high, a high percentage of these whales were feeding (Figure 14). Observations in other years were much more variable. We speculate that humpback whales respond to prey availability by moving in and out of the southwestern flank region, leading to a decrease in whale sightings when prey are rare.

Do sand lances respond to NLIWs? We identified sand lance schools with live video in 2008 and 2012. However, sand lance and NLIWs rarely coincided in our acoustic observations, and our data cannot resolve this question. More study is required to address whether sand lance responds to the NLIWs. In the North Sea, *Embling et al*. [2012] found that sand lance *Ammodytes* sp. may respond to tidal currents, with an increase in number of sand lance schools at maximum ebb or flood tides, but no mechanism was invoked, and the response to different phases of the tide were variable. It was suggested that changes in vertical distribution associated with changing tides may offer a foraging opportunity to pelagic birds [*Embling et al*., 2012]. Sand lance might thus change vertical distribution in response to environmental cues. The modeled Race Point waves of depression with amplitude of $\eta_0 = -14$ m, comparable to the observed waves, cause changes in bottom current speed up to about 30 cm/s, and dynamic pressure changes of about 0.8 Pa one meter above the bottom (Figure 11). Sand lance may sense hydrodynamic disturbances caused by the NLIWs, as sand lance respond to hydrodynamic disturbances presumably sensed with their lateral line [*Peterson*, 1984].

NLIWs shoaling might affect positively sand lance habitat by generating currents that affect the ocean bottom. For example, *Noble and Xu* [2003] speculated that coarse sediments at a site in 70–100 m water depths off California resulted from winnowing by internal bore generated currents. Sand lance prefer coarse sediment bottoms [*Meyer et al*., 1979], and their habitat may be positively influenced by semidiurnal NLIWs shoaling, as these events are significant in sediment resuspension [*Butman et al*., 2006; *Quaresma et al*., 2007].

## 5. Summary

To conclude, there was no temporal relationship between the occurrence of whales and NLIWs at the temporal scale of the wave events. One complicating factor in elucidating a temporal correlation between humpback whales and NLIWs is that waves occur regardless of the presence of sand lance and other small fish, and with no prey available, a link between hydrodynamic forcing and whale occurrence is not

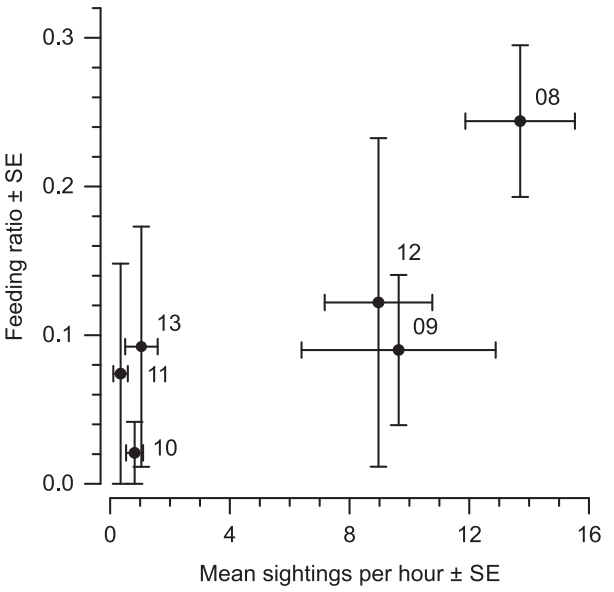


**Figure 14.** Relationship between mean sightings per hour and the feeding ratio. Numbers by data points are years, and error bars are standard error.

expected. At SB's southern flank, there was large interannual variability in whale sightings during the summer, which may relate to prey availability. Factors such as behavior and social cohesion may also influence humpback whale distribution [e.g., *Whitehead and Carlson*, 1988]. Finally, our results indicate that Race Point waves are not in phase with the internal tide, as there was no change on average thermocline depth after passage of the Race Point NLIWs, suggesting that Race Point NLIW transport potential is lower relative to coastal NLIWs that are in phase with the internal tide [*Pineda*, 1999].

Stellwagen Bank's southwestern flank is a hotspot of biological activity in the sense that pelagic prey and predators congregate in the area, and Race Point NLIWs might play a role in the secondary production of the site by contributing with increased zooplankton fluxes or enhancing sand lance habitat. However, these potential contributions by semidiurnal NLIWs have yet to be evaluated, and it is likely that other hydrodynamic processes play more important roles.

**Acknowledgments**

We thank the help and logistical support of Brad Cabe, Danielle Cholewiak, Denise Risch, Jorge Magalhaes, Evelyn Ganson, Bob Caron, Cara Pekarcik, the many Stellwagen Bank National Marine Sanctuary and Woods Hole Oceanographic Institution volunteers, and Captain Bob Wallace, Dave Arch, and the crew of the R/V *Auk*. The detailed comments from two reviewers improved the ms. We would also like to acknowledge funding from the National Oceanic and Atmospheric Administration Sea Grant (Woods Hole), the Woods Hole Oceanographic Institution, the ESA, and the German Aerospace Center. Data used in this study are available by contacting J. Pineda (jpineda@whoi.edu), and Jose da Silva (jdasilva@fc.up.pt) for the SAR data.

## References

Alpers, W. (1985), Theory of radar imaging of internal waves, *Nature*, *314*, 245–247, doi:10.1038/314245a0.

Auster, P., R. Clark, and R. E. S. Reed (2006), Marine fishes, in *An Ecological Characterization of the Stellwagen Bank National Marine Sanctuary Region: Oceanographic, Biogeographic, and Contaminants Assessment, NOAA Tech. Mem. NCCOS 45*, edited by T. Battista, et al., pp. 89–230, U.S. Dep. of Comm., Natl. Ocean. and Atmos. Admin., Natl. Ocean Serv., Natl. Cent. for Coastal Ocean Sci., Silver Spring, Md.

Butman, B., P. S. Alexander, A. Scotti, R. C. Beardsley, and S. P. Anderson (2006), Large internal waves in Massachusetts Bay transport sediments offshore, *Cont. Shelf Res.*, *26*, 2029–2049, doi:10.1016/j.csr.2006.07.022.

Chereskin, T. K. (1983), Generation of internal waves in Massachusetts Bay, *J. Geophys. Res.*, *88*, 2649–2661, doi:10.1029/JC088iC04p02649.

Clapham, P. J., and J. G. Mead (1999), *Megaptera novaeangliae*, *Mamm. Spec.*, *604*, 1–9.

Clark, R., J. Manning, B. Costa, and A. Desch (2006), Physical and oceanographic setting, in *An Ecological Characterization of the Stellwagen Bank National Marine Sanctuary Region: Oceanographic, Biogeographic, and Contaminants Assessment, NOAA Tech. Mem. NCCOS 45*, edited by T. Battista, et al., pp. 1–58, U.S. Dep. of Comm., National Oceanic and Atmospheric Administration, National Ocean Service, National Centers for Coastal Ocean Sci., Silver Spring, Md.

da Silva, J. C. B., and K. R. Helfrich (2008), Synthetic aperture radar observations of resonantly generated internal solitary waves at Race Point Channel (Cape Cod), *J. Geophys. Res.*, *113*, C11016, doi:10.1029/2008JC005004.

da Silva, J. C. B., S. A. Ermakov, I. S. Robinson, D. R. G. Jeans, and S. V. Kijashko (1998), Role of surface films in ERS SAR signatures of internal waves on the shelf. 1. Short-period internal waves, *J. Geophys. Res.*, *103*, 8009–8031, doi:10.1029/97JC02725.

Dawbin, W. H. (1966), The seasonal migratory cycle of humpback whales, in *Whales, Dolphins and Porpoises*, edited by K. S. Norris, pp. 145–170, Univ. of Calif. Press, Berkeley, Calif.

DiBacco, C., H. Fuchs, J. Pineda, and K. Helfrich (2011), Swimming behavior and velocities of barnacle cyprids in a downwelling flume, *Mar. Ecol. Prog. Ser.*, *433*, 131–148, doi:10.3354/meps09186.

Embling, C. B., J. Illian, E. Armstrong, J. van der Kooij, J. Sharples, K. C. J. Camphuysen, and B. E. Scott (2012), Investigating fine-scale spatio-temporal predator–prey patterns in dynamic marine ecosystems: A functional data analysis approach, *J. Appl. Ecol.*, *49*(2), 481–492, doi: 10.1111/j.1365–2664.2012.02114.x.

Embling, C. B., J. Sharples, E. Armstrong, M. R. Palmer, and B. E. Scott (2013), Fish behaviour in response to tidal variability and internal waves over a shelf sea bank, *Prog. Oceanogr.*, *117*, 106–117, doi:10.1016/j.pocean.2013.06.013.

Franks, P. J. S. (1992), Sink or swim: Accumulation of biomass on fronts, *Mar. Ecol. Prog. Ser.*, *82*, 1–12.

Friedlaender, A. S., E. L. Hazen, D. P. Nowacek, P. N. Halpin, C. Ware, M. T. Weinrich, T. Hurst, and D. Wiley (2009), Diel changes in humpback whale *Megaptera novaeangliae* feeding behavior in response to sand lance *Ammodytes* spp. behavior and distribution, *Mar. Ecol. Prog. Ser.*, *395*, 91–100, doi:10.3354/meps08003.

Garrison, L. P., and J. S. Link (2000), Fishing effects on spatial distribution and trophic guild structure of the fish community in the Georges Bank region, *ICES J. Mar. Sci.*, *57*(3), 723–730.

Hain, J. H. W., G. R. Carter, S. D. Kraus, C. A. Mayo, and H. E. Winn (1982), Feeding behavior of the humpback whale, *Megaptera novaeangliae*, in the western North-Atlantic, *Fish. Bull.*, *80*(2), 259–268.

Halpern, D. (1971), Observations on short-period internal waves in Massachusetts Bay, *J. Mar. Res.*, *29*, 116–132.

Hamner, W. M. (1988), The "lost year" of the sea turtle, *Trends Ecol. Evol.*, *3*, 116–118, doi:10.1016/0169–5347(88)90120-6.

Haury, L. R., M. B. Briscoe, and M. H. Orr (1979), Tidally generated internal wave packets in Massachusetts Bay, *Nature*, *278*, 312–317, doi:10.1038/278312a0.

Haury, L. R., P. H. Wiebe, M. H. Orr, and M. G. Briscoe (1983), Tidally generated high-frequency wave packets and their effect on plankton in Massachusetts Bay, *J. Mar. Res.*, *41*, 65–112.

Hazen, E. L., A. S. Friedlaender, M. A. Thompson, C. R. Ware, M. T. Weinrich, P. N. Halpin, and D. N. Wiley (2009), Fine-scale prey aggregations and foraging ecology of humpback whales *Megaptera novaeangliae*, *Mar. Ecol. Prog. Ser.*, *395*, 75–89, doi:10.3354/meps08108.

Helfrich, K. R., and J. Pineda (2003), Accumulation of particles in propagating fronts, *Limnol. Oceanogr.*, *48*, 1509–1520.

Helfrich, K. R., and B. L. White (2010), A model for large-amplitude internal solitary waves with trapped cores, *Nonlin. Proc. Geophys.*, *17*(4), 303–318, doi:10.5194/npg-17–303-2010.

Kingsford, M. J., and J. H. Choat (1986), Influence of surface slicks on the distribution and onshore movements of small fish, *Mar. Biol. (Berl.)*, *91*, 161–171.

Lai, Z., C. S. Chen, G. W. Cowles, and R. C. Beardsley (2010a), A nonhydrostatic version of FVCOM: 2. Mechanistic study of tidally generated nonlinear internal waves in Massachusetts Bay, *J. Geophys. Res.*, *115*, C12049, doi:10.1029/2010JC006331.

Lai, Z., C. Chen, R. C. Beardsley, B. Rothschild, and R. Tian (2010b), Impact of high-frequency nonlinear internal waves on plankton dynamics in Massachusetts Bay, *J. Mar. Res.*, *68*, 259–281, doi:10.1357/002224010793721415.

Lamb, K. (1997), Particle transport by nonbreaking, solitary internal waves, *J. Geophys. Res.*, *102*, 18,641–18,660, doi: 10.1029/97JC00441.

Lamb, K. (2002), A numerical investigation of solitary internal waves with trapped cores formed via shoaling, *J. Fluid Mech.*, *451*, 109–144, doi:10.1017/S002211200100636X.

Le Fèvre, J. (1986), Aspects of the biology of frontal systems, *Adv. Mar. Biol.*, *23*, 163–299.

Leichter, J. J., G. Shellenbarger, S. J. Genovese, and S. L. Wing (1998), Breaking internal waves on a Florida coral reef: A plankton pump at work?, *Mar. Ecol. Prog. Ser.*, *166*, 83–97.

Lennert-Cody, C., and P. J. S. Franks (1999), Plankton patchiness in high-frequency internal waves, *Mar. Ecol. Prog. Ser.*, *186*, 59–66.

Meyer, T. L., R. A. Cooper, and R. W. Langton (1979), Relative abundance, behavior and food habits of the American sand lance, *Ammodytes americanus*, from the Gulf of Maine, *Fish. Bull.*, *77*, 243–253.

Moore, S. M., and R.-C. Lien (2007), Pilot whales follow internal solitary waves in the South China Sea, *Mar. Mamm. Sci.*, *23*, 193-196.

Nelson, T. A., and B. Boots (2008), Detecting spatial hot spots in landscape ecology, *Ecography*, *31*(5), 556–566, doi:10.1111/j.0906–7590.2008.05548.x.

Noble, M., and J. P. Xu (2003), Observations of large amplitude cross-shore internal bores near the shelf break, Santa Monica Bay, CA, *Mar. Env. Res.*, *56*, 127–149, doi:10.1016/S0141-1136(02)00328-8.

Payne, P. M., D. Wiley, S. Young, S. Pittman, P. J. Clapham, and J. W. Jossi (1990), Recent fluctuations in the abundance of baleen whales in the southern Gulf of Maine in relation to changes in prey abundance, *Fish. Bull.*, *88*, 687–696.

Peterson, D. E. (1984), Sensitivity to hydrodynamic stimuli and predator detection in the American sand lance, *Ammodytes americanus* (Pisces: Ammodytidae), MS thesis, Long Island Univ, Brookville, N. Y.

Pineda, J. (1994), Internal tidal bores in the nearshore: Warm-water fronts, seaward gravity currents and the onshore transport of neustonic larvae, *J. Mar. Res.*, *52*, 427–458.

Pineda, J. (1999), Circulation and larval distribution in internal tidal bore warm fronts, *Limnol. Oceanogr.*, *44*, 1400–1414.

Quaresma, L. S., J. Vitorino, A. Oliveira, and J. C. B. da Silva (2007), Evidence of sediment resuspension by nonlinear internal waves on the western Portuguese mid-shelf, *Mar. Geol.*, *246*(2–4), 123–143, doi:10.1016/j.margeo.2007.04.019.

Robards, M. D., M. F. Wilson, R. H. Armstrong, and J. F. Piatt (1999), *Sand Lance: A Review of Biology and Predator Relations and Annotated Bibliography, Res. Pap. PNW-RP 521*, US Dep. of Agric., Forest Serv., Pacific Northwest Res. Stn., Juneau, Alaska.

Scotti, A., and J. Pineda (2004), Observation of very large and steep internal waves of elevation near the Massachusetts coast, *Geophys. Res. Lett.*, *31*, L22307, doi:10.1029/2004GL021052.

Scotti, A., and J. Pineda (2007), Plankton accumulation and transport in propagating nonlinear internal fronts, *J. Mar. Res.*, *65*, 117–145, doi:10.1357/002224007780388702.

Scotti, A., R. C. Beardsley, and B. Butman (2007), Generation and propagation of nonlinear internal waves in Massachusetts Bay, *J. Geophys. Res.*, *112*, C10001, doi:10.1029/2007JC004313.

Scotti, A., R. C. Beardsley, B. Butman, and J. Pineda (2008), Shoaling of nonlinear internal waves in Massachusetts Bay, *J. Geophys. Res.*, *113*, C08031, doi:10.1029/2008JC004726.

Shanks, A. L. (1983), Surface slicks associated with tidally forced internal waves may transport pelagic larvae of benthic invertebrates and fishes shoreward, *Mar. Ecol. Prog. Ser.*, *13*, 311–315.

Stastna, M., and K. G. Lamb (2002), Large fully nonlinear internal solitary waves: The effect of background current, *Phys. Fluids*, *14*(9), 2987–2999, doi:10.1063/1.1496510.

Stevick, P. T., L. S. Incze, S. D. Kraus, S. Rosen, N. Wolff, and A. Baukus (2008), Trophic relationships and oceanography on and around a small offshore bank, *Mar. Ecol. Prog. Ser.*, *363*, 15–28.

U.S. Department of Commerce (2010), *Stellwagen Bank National Marine Sanctuary Final Management Plan and Environmental Assessment*, U.S. Dep. of Comm., Natl. Oceanic and Atmos. Admin., Off. of Natl. Mar. Sanctuaries, Silver Spring, Md.

Vargas, C. A., D. A. Narváez, A. Piñonez, R. Venegas, and S. A. Navarrete (2004), Internal tidal bore warm fronts and settlement of invertebrates in Central Chile, *Estuar. Coast. Shelf Sci.*, *61*, 603–612, doi:10.1016/j.ecss.2004.07.006.

Ware, C., D. N. Wiley, A. S. Friedlaender, M. Weinrich, E. L. Hazen, A. Bocconcelli, S. E. Parks, A. K. Stimpert, M. A. Thompson, and K. Abernathy (2014), Bottom side-roll feeding by humpback whales (*Megaptera novaeangliae*) in the southern Gulf of Maine, U.S.A, *Mar. Mamm. Sci.*, *30*(2), 494–511, doi:10.1111/mms.12053.

Watkins, W. W., and W. E. Schevill (1979), Aerial observation of feeding behavior in four baleen whales: *Eubalaena glacialis*, *Balaenoptera borealis*, *Megaptera novaeangliae*, and *Balaenoptera physalus*, *J. Mamm.*, *60*, 155–163.

Weinrich, M., and A. E. Kuhlberg (1991), Short-term association patterns of humpback whale (*Megaptera novaeangliae*) groups on their feeding grounds in the southern Gulf of Maine, *Can. J. Zool.*, *69*, 3005–3011.

Weinrich, M., M. Schilling, and C. R. Belt (1992), Evidence for acquisition of a novel feeding behaviour: Lobtail feeding in humpback whales, *Megaptera novaeangliae*, *Anim. Behav.*, *44*, 1059–1072.

Weinrich, M., M. Martin, R. Griffiths, J. Bove, and M. Schilling (1997), A shift in distribution of humpback whales, *Megaptera novaeangliae*, in response to prey in the southern Gulf of Maine, *Fish. Bull.*, *95*, 826–836.

Whitehead, H., and C. Carlson (1988), Social behavior of feeding finback whales off Newfoundland: Comparisons with the sympatric humpback whale, *Can. J. Zool.*, *66*(1), 217–221.

Wiley, D., J. C. Moller, and K. A. Zilinskas (2003), The distribution and density of commercial fisheries and baleen whales within the Stellwagen Bank National Marine Sanctuary: July 2001–June 2011, *Mar. Tech. Soc. J.*, *37*(1), 35–53, doi:10.4031/002533203787537384.

Wiley, D., C. Ware, A. Bocconcelli, D. Cholewiak, A. Friedlaender, M. Thompson, and M. Weinrich (2011), Underwater components of humpback whale bubble-net feeding behaviour, *Behaviour*, *148*(5-6), 575–602.

Winant, C. D., and A. Bratkovich (1981), Temperature and currents in the southern California shelf: A description of the variability, *J. Phys. Oceanogr.*, *11*, 71–86, doi:10.1175/1520-0485(1981)011<0071:TACOTS>2.0.CO;2.

Witman, J. D., J. J. Leichter, S. J. Genovese, and D. A. Brooks (1993), Pulsed phytoplankton supply to the rocky subtidal zone: Influence of internal waves, *Proc. Natl. Acad. Sci. U. S. A.*, *90*, 1686–1690, doi:10.1073/pnas.90.5.1686.

Zeldis, J. R., and J. B. Jillet (1982), Aggregation of pelagic *Munida gregaria* (Fabricius) (Decapoda, Anomura) by coastal fronts and internal waves, *J. Plankton Res.*, *4*, 839–857.[10.1093/plankt/4.4.839].